

## INVESTIGATION OF OPTICAL INHOMOGENEITIES IN THREE-ELECTRODE DISCHARGE XeCl-LASER

A.V. Andramanov, V.V. Borovkov, and S.L. Voronov

*Federal Nuclear Center of Russia,  
the All-Russian Scientific-Research Institute for Experimental Physics,  
Sarov, Nizhegorodskaya Region  
Received October 9, 1997*

*We present here an experimental investigation into the optical inhomogeneities that may appear in a three-electrode, dual discharge XeCl-laser operated in the regime with pre-multiplication of electrons. Different discharge behaviors in two laser channels have been revealed and explained. It was found that the onset of output power fall off correlates with the development of discharge instabilities. Based on the data obtained the conclusion about the development and evolution of filamentous channels in the discharge plasma is drawn.*

### 1. INTRODUCTION

Great progress in the discharge lasers is associated with the development of dual discharge schemes or the so-called pre-pulse technique (see Refs. 1–3). In this method of active medium excitation a short, high-voltage, and low-energy pulse forms the discharge while the major portion of the pump energy is deposited from another capacitive storage unit. The lower charging voltage of the storage unit provides for better matching between the pump source impedance and the load. Schemes of dual discharge in two-electrode excimer lasers are realized using a magnetic switch in the circuit of the main capacitive storage unit. Thus, the record efficiency of 5% was reported in Ref. 4 for a single-pulse XeCl-laser with a magnetic switch. Pulse-periodic laser with the average output power of 1.5 kW and efficiency of 2.2% was described in Ref. 5.

Other method of the dual-discharge formation is realized in three-electrode lasers. Therewith, the capacitive storage units are coupled to outer electrodes while the discharge is formed by a high-voltage control pulse applied to the central electrode (see Refs. 6–9).

If charging voltage of the main pumping source is decreased, its capacitance should be increased to maintain the specific energy deposition. As a result, the pumping pulse duration increases. However, it is known that the discharge in halogen containing mixtures loses its stability with time. At the moment two mechanisms of the instability development in active media of excimer lasers have been proposed. These are the step-wise ionization instability of plasma (see Ref. 10) and the halogen donor “burning out” (see Ref. 11). The mechanism of attaching-vibrational discharge stabilization has been described in Ref. 12.

Experimental investigation presented in Ref. 13 shows that during the pump pulse there occurs a fall

off of the emission power followed by termination of lasing when thin filaments appear against the background of a diffuse discharge.

Up to now, the experimental investigations of XeCl lasers were aimed at study of the effect of preionization conditions, gas mixture composition, and pump power on the lasing properties. To obtain a more detailed information on the optical quality of the active media and on the development of instabilities in plasma one has to use interference methods of the discharge investigations.

The experimental study of optical inhomogeneities (OI), in a three-electrode XeCl-laser with dual discharge, made using interferometric methods is discussed in this paper. In this study we have measured temporal and spatial distributions of the electron number density in the discharge plasma and revealed small-scale gas-dynamic optical inhomogeneities (SSOI).

### 2. EXPERIMENTAL SETUP AND MEASUREMENT PROCEDURE

Three-electrode XeCl laser described in Ref. 9 was used in our experiments. The electrodes with Chang profile form two discharge gaps of 3.5 cm each. The active length was 50 cm, and the discharge width estimated on the output radiation spot was about 2 cm. To provide initial electrons we have used two-side arc preionization. The gaps undergo the electric breakdown one after the other, as a high-voltage low-energy pulse is successively applied to the central control electrode. The gaps, according to the time of their breakdown are called the first and second channels, respectively. Total capacitance of the capacitor connected to the outer electrodes and assembled as a two-polarity power supply was 0.32  $\mu\text{F}$ , and the discharge circuit inductance was about 50 nH. The capacitive storage unit of the main discharge was charged to  $\pm 10$  kV from a two-polarity

power supply. The capacitor of driving circuit was charged from a separate dc power supply to a voltage up to 28 kV. Oscilloscope traces of the discharge current and laser pulses in the two channels are shown in Fig. 1. The current pre-pulse in the first channel is caused by charging of the peaking capacitors in the discharge formation circuit. The discharge was studied in the gas mixture of Ne:Xe:HCl at partial pressures of 4 atm, 12 Torr, and 1.2 Torr.

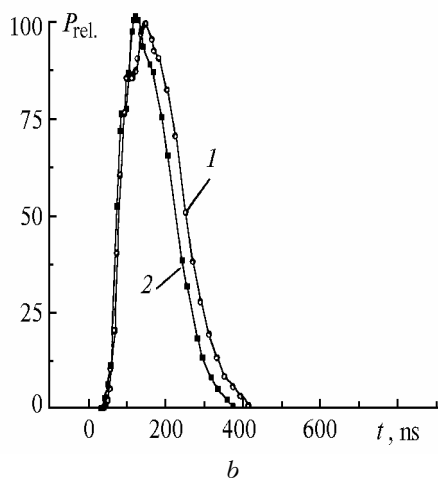
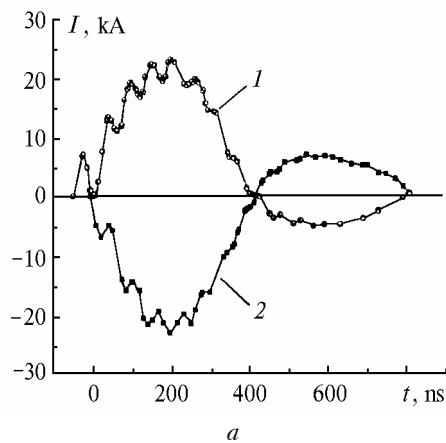


FIG. 1. Oscilloscope traces of the discharge current and laser pulses in two channels of the laser.

The OI were studied using a Michelson interferometer at the wavelength of He-Ne laser (633 nm). Reference experiments performed with the use of an argon-ion laser (514 nm) demonstrate that free plasma electrons make major contribution to changes in the refractive index ( $\Delta n$ ). This is in agreement with the data presented in Ref. 14. The interference patterns were recorded by a high-speed camera SFR operating in the slot scan mode with time resolution of 30 ns. Two position of the slot, namely, parallel or normal to the electrode plane were used in the OI measurements. The changes of  $\Delta n$  were measured with an accuracy no less than  $3.2 \cdot 10^{-8}$  which corresponds to electron concentration  $N_e = 1.8 \cdot 10^{14} \text{ cm}^{-3}$ .

### 3. EXPERIMENTAL RESULTS AND DISCUSSION

In the present paper, our primary attention has been paid to the study of the effect of pumping power and peculiarities of the discharge formation in a three-electrode laser, on the development of plasma instabilities. Figure 2 depicts characteristic interferograms of OI in the laser channels. The results of the interferograms processing are presented in Figs. 3 and 4. Figure 3 shows the dependence  $N_e(t)$  in different channels. Two stages characteristic of  $N_e$  variation have been revealed in our experiments. Slow increase of electron density in the channels up to  $(1-2) \cdot 10^{15} \text{ cm}^{-3}$  correlating with the discharge current rise is evident during the first stage (see Figs. 3a and b). These variations of  $N_e(t)$  are typical for diffuse discharge (see Ref. 15). Sharp electron multiplication starting from 160 to 170 ns and most evident in the second channel corresponds to the other stage. Similar behavior of the electron concentration growth in the center of a XeCl-laser discharge with the duration of 250 ns was noticed in Ref. 14. The discontinuity of the growth at 70 ns was explained by development of the discharge instabilities.

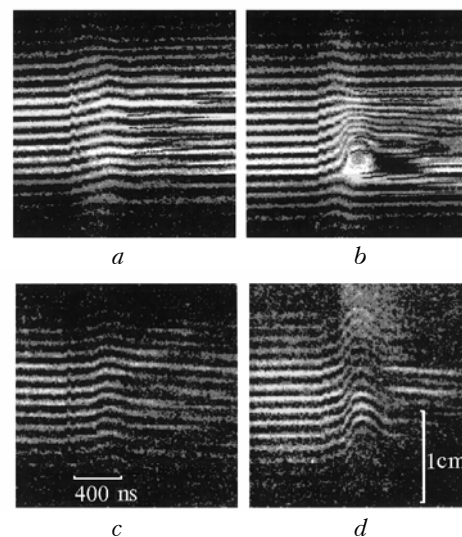


FIG. 2. Interferograms of the optical inhomogeneities in the first (a, c) and second (b, d) laser channels. The slit of the fast camera is parallel (a, b) and normal (c, d) to the electrodes.

It is seen from the interferograms (see Figs. 2a and b) that when electron concentration in the second channel decreases, splitting of the interference fringes caused by SSOI formation is evident in this discharge region after 330 ns. Much weaker splitting was observed in the first channel either, but only by 400 to 450 ns. The fact that the splitting is observed after the current pulse termination (see Figs. 2a and b), when the electron number density has already relaxed, along with the estimation made from the time of appearance of the splitting and its development dynamics, allows

us to conclude that small-scale inhomogeneities of the refractive index are caused by gas dynamic dumping of filamentous current channels that appear at the moment when the rate of the electron density rapidly increases. The initial size of these OIs was recorded to be 0.3 to 0.35 mm.

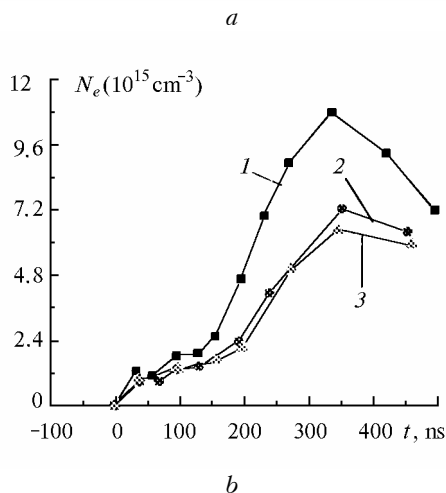
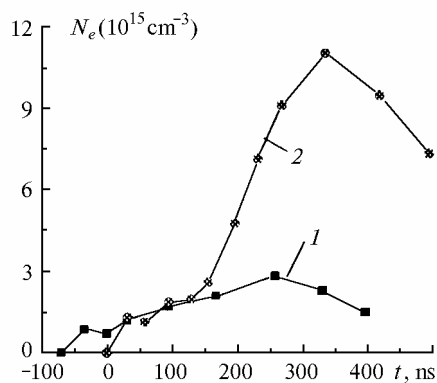


FIG. 3. The electron number density in the discharge plasma,  $N_e$ , as a function of time in the first (a; curve 1) and second (curve 2) channels and in the center of the second channel (b) at 9 kV (curve 1), 8 kV (curve 2) and 7.5 kV (curve 3).

As noted in Refs. 13 and 16, formation of the discharge instabilities is associated with the near-electrode processes, in particular, with the explosion of cathode spots followed by the development of high-current channels within these spots. This phenomenon has also been observed in our experiments. It is seen from Fig. 2c and d (the slit is normal to the electrode plane) that the onset of a sharp increase of  $N_e$  is accompanied by the appearance of a bright region in the vicinity of the cathode which then extends for 5–7 mm toward the anode and by enhancement of the discharge emission in the visible spectral range. It is evident that this is caused by explosion of cathode spots and intergrowth of high-current channels. The presence of incomplete streamers near the cathode was detected visually, as well.

It is likely that the growth of the electric field strength at the heads of near-cathode channels results in the initiation of the ionization wave propagating at a rate about  $10^8$  cm/s (see Ref. 17) and in formation of high-current microchannels of an enhanced electron density. Then, current redistributes from the diffuse discharge regions into the channel zones and dumping of filamentous channels appearing as SSOI development takes place. Theoretical analysis of the filamentous instability development in the discharge was performed in Ref. 12.

From our experiments we have revealed the effect which the filamentous current channels and their SSOI appearing due to the gas dynamic dumping show on the performance parameters of the XeCl-laser. As is seen from Fig. 1, the fall off of the output power in the second channel starting at ~160 ns coincides, in time, with the filament occurrence at that point. There are several causes of such a decrease in the output power. One of the causes is redistribution of the deposited energy between the diffuse discharge regions, where efficient formation of exciplex molecules occurs, and the filamentous channels. Build up of absorption in the regions with an enhanced electron density, where the formation of absorbing complexes is highly efficient (see Ref. 15), also contributes into that process. Termination of lasing in the second channel occurred by 350 ns that coincides, in time, with the rise of SSOI introducing additional refractive losses into the resonator. The fall off of laser power in the first channel began later than in the second one while the output pulse duration was equal to half-period of the discharge current. It should be noted that the output energy in the first channel was also higher than that in the second one.

As mentioned above, large-scale variations of the refractive index during the discharge are caused by free electrons in plasma. Figure 4 depicts the distribution  $N_e(x)$  over the discharge cross section at different moments in time. It is seen that by the moment, when total discharge current forms (0 ns) there is a double-peak electron density distribution formed in the first channel. The reason for this is that during the breakdown (–35 ns) in the first gap a bell-shaped distribution of electron density forms following the transverse distribution of the electric field strength there. This, in turn, provides for a higher rate of formation of vibrationally excited HCl molecules in the discharge center. It is known that the cross-section of electron dissociative attachment is much higher, when vibrationally exciting HCl molecules (see Ref. 12). Therefore, during a pre-pulse current decay the rate of the dissociative attachment in the discharge center is higher than that at its periphery that results in the development of double-peak distribution of the electron density and in an increase in the discharge half-width. Earlier similar effect was discussed in Refs. 18 and 19 where the laser parameters had been being analyzed. At the same time, the electron density distribution formed in the second laser channel had only one peak at the

gap center. Therewith character of  $N_e(x)$  in both channels does not change during the entire pump pulse. It is seen from Fig. 4 that at the diffuse stage (0 to 170 ns) half-width of discharge in the first channel comprises 70–80% of that in the first one. Then, both discharges gradually contract to the center of the second channel and to the region with the peak value of  $N_e(x)$  in the second one. Minimal discharge width in the second channel formed by ~250 ns comprises ~40% of that in the first one at the same moment.

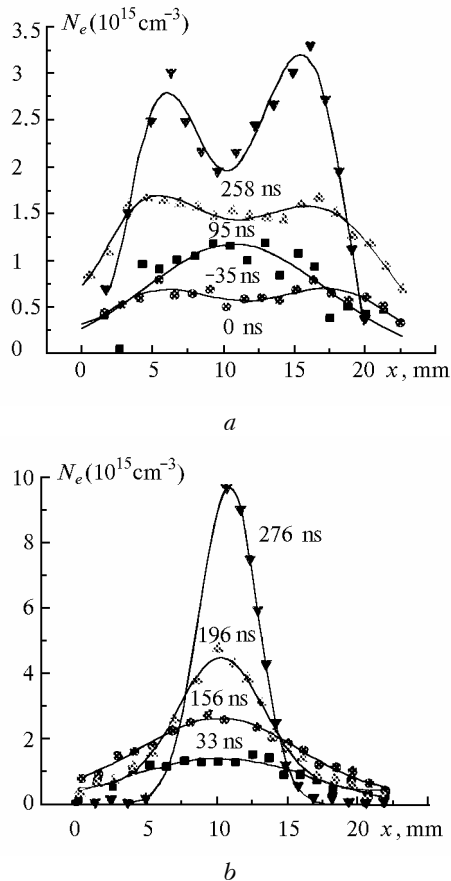


FIG. 4. The electron density distribution over the discharge cross section in the first (a) and second (b) channels.

As seen from Fig. 3 the electron density in the regions with  $N_e(x)$  peaks continues to increase after 200 ns, while the discharge current (see Fig. 1) and pump power decrease. At the same time the integral of electron concentration over the discharge cross section, in the second channel, still increases despite the discharge narrowing (see Fig. 4b). The above results suggest that it is just the development of instabilities that causes the discharge contraction and anomalous growth the electron density in the peaks of  $N_e(x)$  distribution. No increase in the integral electron density during the discharge current decay was observed in the first channel.

The effect of energy deposition and charging voltage of the main capacitive storage unit on the  $N_e(t)$  evolution is seen in Fig. 3. It was found experimentally that, if conditions for the discharge formation are optimal, the variation in energy deposition has only little effect on the discharge width. Thus, it is clear that the discharge current density is determined by energy deposited into the discharge. Its decrease results both in time extension of the diffuse discharge stage and in reducing of  $N_e$  growth in the gap center during the discharge contraction.

#### 4. CONCLUSIONS

Thus, certain regularities in the discharge evolution have been revealed in the course the experiments discussed. The differences observed in the discharge behavior in two laser gaps are explained. It was found that the decrease in the output power correlates with the development of discharge instabilities. The conclusion about formation and growth of filamentous channels in the discharge plasma was drawn based on the obtained data. This results in the redistribution of deposited energy between these filaments and diffuse discharge zones thus decreasing the efficiency of exciplex molecules formation. It was also shown that a decrease in the current density extends both the diffuse stage and the laser pulse duration as well as improves the discharge homogeneity. Splitting of the interference fringes due to the gas dynamic dumping of the filaments was observed at the final discharge stage.

#### REFERENCES

1. W.H. Long, M.J. Plummer, and E.A. Stappaerts, *Appl. Phys. Lett.* **43**, 735–737 (1983).
2. R.S. Taylor, K.E. Leopold, *ibid.* **46**, 335–337 (1985).
3. C.H. Fisher, M.J. Kushner, T.E. De Hart, J.P. McDaniel, and J.J. Ewing, *Appl. Phys. Lett.* **48**, 1574 (1986).
4. J.V. Gerritsen, A.L. Keet, G.J. Ernst, and W.J. Witteman, *Opt. Commun.* **77**, 395–396 (1990).
5. S. Fujikawa, M. Inoue, Y. Sato, K. Haruta, Y. Murai, and H. Nagai, in: *Proceedings of CLEO'94 Conference Digest* (1994), pp. 26–27.
6. S. Bollanti, R. Di Lazzardo, F. Flora, G. Giordano, T. Letardi, C. Petrucci, G. Schina, and C.E. Zhen, *Proc. SPIE* **2206**, 144–153 (1994).
7. V.V. Borovkov, V.V. Voronin, S.L. Voronov, D.I. Zenkov, B.V. Lazhintsev, V.A. Nor-Arevyan, V.A. Tananakin, and G.I. Fedorov, *Kvant. Elektron.* **22**, No. 5, 439–440 (1995).
8. V.V. Borovkov, V.V. Voronin, S.L. Voronov, D.I. Zenkov, B.V. Lazhintsev, V.A. Nor-Arevyan, V.A. Tananakin, and G.I. Fedorov, *Pis'ma Zh. Tech. Fiz.* **21**, No. 4, 36–39 (1995).

9. V.V. Borovkov, V.V. Voronin, B.V. Lazhintsev, V.A. Nor-Arevyan, and G.I. Fedorov, *Atmos. Oceanic Optics* **11**, No. 2-3, 116-119 (1998).
10. V.M. Borisov, V.P. Novikov, and O.B. Khristoforov, *Teplofiz. Vys. Temp.* **24**, No.6, 1072-1078 (1986).
11. J. Gutts and C.E. Webb, *J. Appl. Phys.* **59**, No. 3, 704-710 (1986).
12. A.V. Dem'ianov, I.V. Kochetov, A.P. Napartovich, M. Kapitelli, and S. Longo, *Kvant. Elektron.* **22**, No. 7, 673-682 (1995).
13. R.S. Taylor, *Appl. Phys.* **B41**, 1-24 (1986).
14. S. Chroba, W. Botticher, *ibid.* **51**, 379-385 (1990).
15. V.Yu. Baranov, V.M. Borisov, and Yu.Yu. Stepanov, *Discharge Excimer Lasers on Rare Gas Halides* (Energoatomizdat, Moscow, 1988), 216 pp.
16. Yu.D. Korolev and G.A. Mesyats, *Physics of Pulsed Gas Breakdown* (Nauka, Moscow, 1991), 223 pp.
17. A.N. Lagar'kov and I.M. Rutkevich, *Waves of Electric Breakdown in Confined Plasma* (Nauka, Moscow, 1989), 205 pp.
18. F.A. Van Goor, J.C.M. Timmermans and W.J. Witteman, *Opt. Commun.* **124**, 56-62 (1996).
19. V.M. Baginskii, N.S. Belokrinitskii, P.M. Golovinskii, A.N. Panchenko, V.F. Tarasenko, and A.I. Shchedrin, *Kvant. Elektron.* **17**, No. 11, 1390-1394 (1990).